10.1038/s41550-023-02053-2

A reproduction of the Milky Way's Faraday rotation measure map in galaxy simulations from global to local scales

Stefan Reissl[1]*, Ralf S. Klessen[1,2], Eric W. Pellegrini[3], Daniel Rahner[1], Rüdiger Pakmor[3], Robert Grand[4], Facundo Gómez[5,6], Federico Marinacci[7], and Volker Springel[3]

July 12, 2023

[1]Universität Heidelberg, Zentrum für Astronomie, Institut für Theoretische Astrophysik, Albert-Ueberle-Str. 2, 69120 Heidelberg, Germany
[2]Universität Heidelberg, Interdisziplinäres Zentrum für Wissenschaftliches Rechnen,Im Neuenheimer Feld 205, 69120 Heidelberg, Germany
[3]Max-Planck-Institut für Astrophysik, Karl-Schwarzschild-Str. 1, 85748 Garching, Germany
[4]Astrophysics Research Institute, Liverpool John Moores University, 146 Brownlow Hill, Liverpool, L3 5RF, UK
[5]Instituto de Investigación Multidisciplinar en Ciencia y Tecnología, Universidad de La Serena, Raúl Bitrán 1305, La Serena, Chile
[6]Departamento de Física y Astronomía, Universidad de La Serena, Av. Juan Cisternas 1200 Norte, La Serena, Chile
[7]Institute for Theory and Computation, Harvard-Smithsonian Center for Astrophysics, 60 Garden Street, Cambridge, MA 02138, USA

Magnetic fields are of critical importance for our understanding of the origin and long-term evolution of the Milky Way. This is due to their decisive role in the dynamical evolution of the interstellar medium (ISM) and their influence on the star-formation process [22, 11, 13, 4]. Faraday rotation measures (RM) along many different sightlines across the Galaxy are a primary means to infer the magnetic field topology and strength from observations [23, 24, 40, 15]. However, the interpretation of the data has been hampered by the failure of previous attempts to explain the observations in theoretical models and to synthesize a realistic multi-scale all-sky RM map [3, 7, 27]. We here utilize a cosmological magnetohydrodynamic (MHD) simulation of the

*E-mail: reissl@uni-heidelberg.de

formation of the Milky Way, augment it with a novel star cluster population synthesis model for a more realistic structure of the local interstellar medium [31, 29], and perform detailed polarized radiative transfer calculations on the resulting model [5, 33]. This yields a faithful first principles prediction of the Faraday sky as observed on Earth. The results reproduce the observations of the Galaxy not only on global scales, but also on local scales of individual star-forming clouds. They also imply that the Local Bubble [1, 42] containing our Sun dominates the RM signal over large regions of the sky. Modern cosmological MHD simulations of the Milky Way's formation, combined with a simple and plausible model for the fraction of free electrons in the ISM, explain the RM observations remarkably well, thus indicating the emergence of a firm theoretical understanding of the genesis of magnetic fields in our Universe across cosmic time.

Magnetic fields significantly influence the kinematical and morphlogical properties of the ISM and contribute to regulating the birth of new generations of stars [18]. To better understand this connection, several observational techniques have been developed and perfected over the last century. For example, dust polarization measurements of aligned dust grains [2, 30] and synchrotron emission [4, 20, 35] allow us to infer the projected line-of-sight (LOS) field orientation, while estimates of the LOS field strength can be obtained from the Zeeman effect [9]. However, these methods are only applicable to a limited set of parameters [5], and additional uncertainties arise from our incomplete understanding of the microphysics involved such as grain alignment mechanisms [2]. A complementary approach is to determine the characteristic Faraday rotation measure (RM). It is based on the fact that polarized radiation can change its polarization angle as it passes though a magnetized and ionized medium. The observed signal depends on the magnetic field strength and direction as well as on the density of free electrons, and on the radiation frequency [37].

Since the early 1960's, numerous attempts were made to reconstruct an all-sky RM map of the Milky Way [23, 24, 40] from observations of pulsars and extragalactic background sources. Complementary synthetic data has proven its worth for systematically interpreting and analyzing this plethora of observations [3, 7, 27]. However, all existing approaches are hampered by the fact that the distribution of thermal electrons as well as the detailed structure of the magnetic field are not well known. While the large-scale properties are usually well constrained [25, 14], crucial information about individual star-forming regions and clouds is missing, which is needed to reproduce the observed small-scale features.

Our approach goes beyond the current state-of-the-art and employs data from a high-resolution cosmological simulation to reconstruct the large-scale properties of the galaxy combined with a novel star cluster population synthesis model, which introduces the missing small-scale physics. Specifically, we take the Au-6 galaxy from the Auriga project [12], which is able to reproduce the global star-formation rate and structure of the Milky Way very well, while at the same time predicting the

amplification of minute primordial magnetic seed fields to micro-Gauss strength over secular timescales. We keep the overall gas density and magnetic field structure, but we discard the original stellar population and distribution of free electrons. We then synthesize a new population of star clusters and calculate the corresponding radiative and mechanical feedback based on the WARPFIELD cloud-cluster evolution method [31, 32]. Next, we obtain the corresponding emission from each cluster across the electromagnetic spectrum [28], use the polarized radiative transfer code POLARIS [34] to build up the spatially varying interstellar radiation field in the galaxy, and from that reconstruct the distribution of free electrons in the ISM, as discussed by Pellegrini and colleagues [29]. Finally, we perform a second POLARIS sweep to calculate synthetic Faraday RM all-sky maps [35] from varying positions within the galaxy.

The total integrated angle of linear polarization for an observer follows as

$$\chi_{\rm obs} = \chi_{\rm source} + RM \times \left(\frac{c}{\nu}\right)^2 , \tag{1}$$

where $\chi_{\rm source}$ is the polarization angle of the source and ν is the observed frequency. The integral

$$RM = \frac{1}{2\pi}\frac{e^2}{m_{\rm e}^2 c^4}\int_0^{s_{\rm obs}} n_{\rm th}(s) B_{||}(s) {\rm d}s \tag{2}$$

defines the rotation measure [6] for the non-relativistic limit along the LOS s towards the observer, c is the speed of light, e and $m_{\rm e}$ are the electron charge and mass, respectively, and $B_{||}$ is the LOS magnetic field component. Altogether we compute high-resolution Faraday RM all-sky maps with a total number of $N = 786,432$ pixels for ten distinct observer positions within the Au-6 galaxy (which we denote P01 - P10). They are placed at roughly the same distance to the galactic center as the Sun (that is at galactocentric radii $8\,{\rm kpc} \leq R \leq 10\,{\rm kpc}$) and are located in a gas density cavity similar to the Local Bubble that defines our own Galactic environment [1, 42], as illustrated in Figure 6 of Pellegrini and colleagues [29]..

The existing RM all-sky maps of the Milky Way are built from an ensemble of extragalactic polarized radio sources. Certain patches of the sky with missing data or with reduced coverage are reconstructed applying Bayesian statistics, and consequently, these regions appear to be smoother than the average. We compare our results with the observed all-sky RM maps presented by Oppermann and collaborators [24] and by Hutschenreuter and colleagues [15], who included a larger source number and employed a more sophisticated reconstruction algorithm (O12 and H22 hereafter). We note that it has recently been pointed out [38] that high RM sightlines may have gone undetected for decades, either from instrumental limitations or from biases in the source selection, and that this introduces a systematic shift of these maps towards low RM values.

Figure 1 shows the O12 and H22 data *(top row)* as well as two synthetic RM maps from the Auriga galaxy *(bottom row)* from one exemplary observers position (P01) at the solar circle. The synthetic map at the left takes the galaxy as is [27],

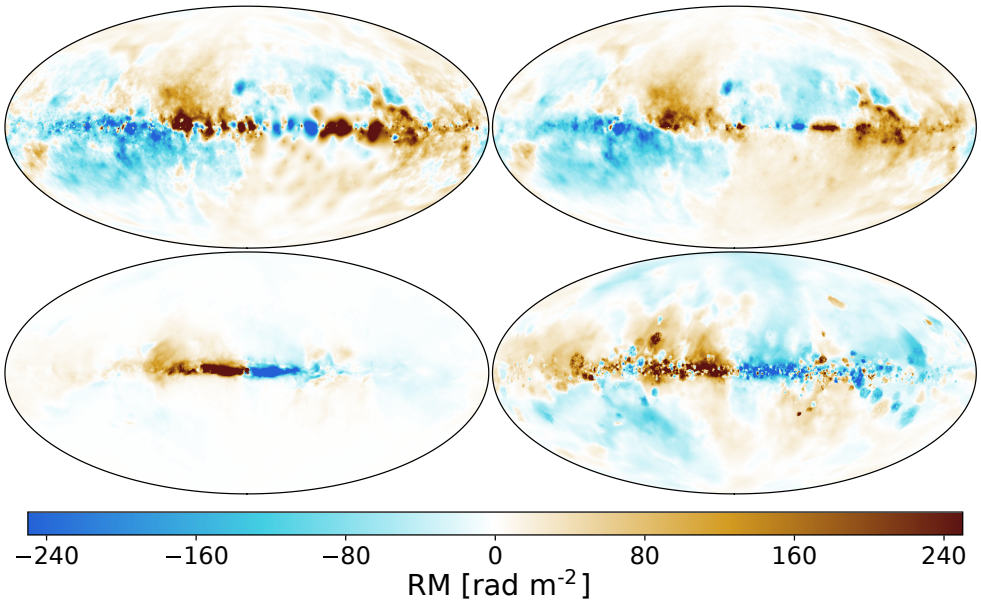

Figure 1: *All-sky Faraday RM map of the Milky Way and of a model galaxy from the Auriga suite of cosmological simulations.* In the top row we show the observed maps of O12 (left) and the data from H22 (right). In the bottom row (left) we provide the synthetic RM map constructed from the original Au-6 data [27]. The lack of signal at large galactic latitudes and the failure to reproduce small-scale features is evident. This problem is remedied by combining the galaxy with a realistic small-scale model of star-cluster formation and evolution and a self-consistent reconstruction of the density of free electrons [29], while keeping the original magnetic field structure of the cosmological simulation [26]. The resulting resulting RM map is shown at the bottom right and very similar to the Milky Way observations.

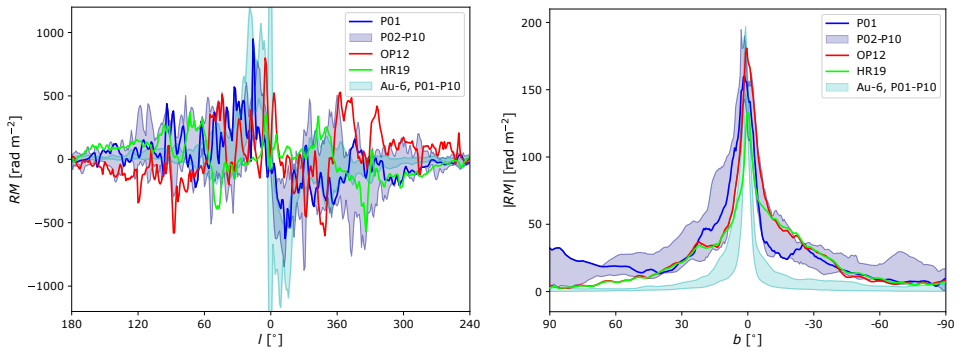

Figure 2: *Average magnitude of the Faraday RM along the Galactic longitude l (left panel) and Galactic latitude b (right panel).* The magnitude of the Faraday RM has been averaged over latitude within $|b| < 1.2^\circ$ when shown as a function of longitude for all of our all-sky RM maps. The amount of RM differs for each of the observer positions (synthetic and our own within the Milky Way) as a result of the local electron distributions and magnetic field directions, respectively. However, all RM profiles show the same trend from positive to negative values at $l = 0^\circ$ as the large scale toriodal field component reverses its direction with respect to the observer. Also, the general synthetic and observed trends agree well with a peak at $b = 0^\circ$ and a minimum towards the poles.

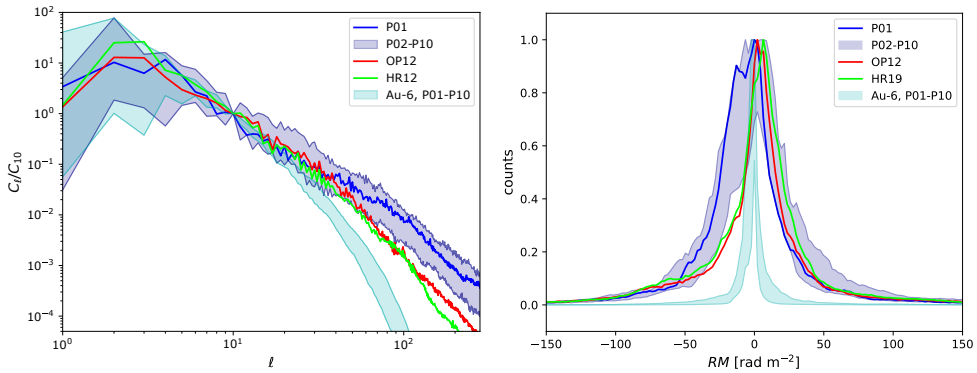

Figure 3: *Multipole spectrum of RM maps for ten different observer positions compared to observational data for the Milky Way.* Left panel: Direct multipole spectrum as a function of multipole moment ℓ for ten different observer positions (P01-P10) within the origin Au-6 galaxy and our modified galaxy version and compares with the reconstructed RM observational data of O12 and H22. A multipole moment of $\ell = 100$ corresponds roughly to a resolution of 14.4°. At higher ℓ the synthetic map of the modified galaxy shows more structure all over the sky in comparison with the reconstructed O12 and H22 data. All spectra are normalized at $\ell = 10$ for better comparison. Right panel: Histogram of the RM healpix maps shown in Fig. 1. All distributions are normalized by their peak values.

based on the data of the cosmological simulation only, and the right one combines the simulation data with the detailed model for star-cluster formation and evolution [29] described above. It is immediately obvious that the Auriga-only maps misses small-scale features, whereas the full model agrees remarkably well the observations. It has a comparable level of fluctuations on small angular scales and gives the right RM magnitude in all regions of the sky. We also note that all maps exhibit a reversal of the magnetic field direction at the Galactic center, as indicated by a transition from positive to negative RM values. This transition is a distinct feature of the magnetic field morphology of the Milky Way, revealing a globally toroidal field structure. It is also well visible in Figure 2, where we plot the average RM along the Galactic longitude *l (left)* and latitude *b (right)* coordinates for all observer positions in the model galaxy. The field reversal in the center is a global property of the disk and therefore independent of the location of the measurement. Similarly, all models exhibit the highest amount of RM near the disk midplane ($b = 0^\circ$) with decreasing values towards the poles ($b = \pm 90^\circ$), again in agreement with O12 and H22, indicating that the magnetic field quickly decreases further up and down into the Galactic halo. We also mention that our model slightly overestimates the amount of RM at large b with an offset of $0 - 30$ rad m^{-2}. Since the signal at large latitudes b is mostly produced by material that is nearby [27], this deviation emphasizes again the importance of properly accounting for the immediate surrounding of the Sun, and it is an indication of the limitations of current galaxy formation simulations when it comes to reproducing the Local Bubble [1, 42].

For a more quantitative comparison, we compute the multipole expansion of the RM maps and display the result in Figure 3. Our synthetic RM spectra are consistent with the O12 and H22 data for all multipole moments $\ell \lesssim 30$ at all observer positions, whereas we are predicting more small-scale structures at larger ℓ. We speculate that this may be a result of the bias in the Bayesian statistics of O12 and H22 towards lower RM values [38]. In contrast, the expansion of the original AU-6 galaxy [27] deviates from the observations already above $\ell \approx 10$ indicating again importance of small-scale physics for the interpretation of the Milky Way data. We stress that including a realistic star-cluster population synthesis model is indispensable for reproducing the observed small-scale (large ℓ) features. We also note that similar conclusions have been reached by Beck and collaborators [3], however, they did so by introducing a small-scale random magnetic field component still lacking the contribution of a proper multi-scale thermal electron model.

Altogether, we find that the general trends in the RM maps presented here agree well for different positions within the galaxy, and they all reproduce the observed data. Consequently, we conclude that current high-resolution MHD simulations of formation and evolution of the Milky Way in a cosmological context, combined with adequate models of star formation and stellar feedback, can well explain the properties of magnetic fields in spiral galaxies. This marks an important step forward in our theoretical understanding of magnetic field amplification by various forms of the dynamo process acting in these systems [27, 36]. We note that the methods presented here can also be applied to RM observations in the high-redshift

Universe [21] and can thus help to monitor the genesis of magnetic fields over cosmic timescales. However, we also caution that most of the RM signal above and below the Galactic plane might be dominated by the local environment [27]. Subsequently, maps of the Faraday rotation of the Milky Way cannot be adequately interpreted without knowledge of the conditions in our Local Bubble [1, 42]. This has been proposed before [40, 27], and it is also implied by the dust polarization measurements of the Planck satellite [1]. Distinct observers in different parts of the Galaxy would see different local magnetic field configurations and electron densities. Our results suggest that current measurements of the Milky Way RM carry a level of uncertainty that was previously not fully appreciated and that can only be accounted for on a statistical basis by detailed modeling efforts as presented here.

Methods

To construct the synthetic all-sky Faraday RM map of the Milky Way, we take one of the simulations from the Auriga project [12]. The galaxy Au-6 is the result of a very high-resolution cosmological MHD zoom-in simulation from initial conditions that are specifically selected to reproduce key features of the Local Group. The calculation includes line cooling, stellar evolution, galactic winds, and the growth of black holes and their associated AGN feedback [12]. All simulations include self-consistently evolving magnetic fields on a Voronoi grid [25] with the moving mesh code AREPO [39]. The galaxy Au-6 is selected as Milky Way analogue based on its size, total mass, and star formation rate.

In the next step we follow the procedure as outlined by Pellegrini and colleagues [29] (hereafter P21) and synthesize a new cluster population and electron fractions that are more faithful to star-forming physics and small scale density structures know from observations. To do so, we replace the original star particles and electron fractions from the simulation and instead reconstruct this information from first principles employing the WARPFIELD cloud/cluster evolution model [31, 32]. It follows the time evolution and structure of the stellar wind bubble, HII region, and protodissociation region (PDR) surrounding a cluster of massive stars in spherical symmetry. WARPFIELD accounts self-consistently for the physics of stellar winds, supernovae, radiation pressure, ionization, and gravity. It solves explicitly for the density structure adopted by the gas in response to the action of these various feedback processes, and therefore allows one to account for the evolution of the luminosity and emerging spectrum.

We determine the local gas mass within equidistant annuli of the Au-6 galaxy, using linearly spaced radial bins originating at the galactic center-of-mass and sample the cluster mass function by randomly depositing mass with a rate obtained from the Kennicutt-Schmidt [17] relation. Per annulus and cluster a random location is selected. If the total gas mass within a distance less than 50 pc from that location is larger than the cluster mass we have drawn, then the cluster is placed there, and the corresponding gas mass is subtracted from the original Voronoi grid

of the Au-6 galaxy. As a result of this procedure, the star clusters are typically inserted near density peaks. This is consistent with observations, where young clusters are seen in the vicinity of dense molecular gas, but no longer are deeply embedded into their parental clouds due to efficient stellar feedback [19]. This leads to a realistic stellar population that is characterized by the number of clusters for a given mass and age in each annulus. An illustratino of this approach is presented in Figure 6 of P21.

The physical properties of each cluster including all emission properties are obtained from the WARPFIELD database [31, 32] combined with the spectral synthesis code CLOUDY[1] v17.00 [10]. This information [28] is then used to compute the impact of ionizing radiation from each individual cluster on the ambient Galactic ISM in order to (re)populate the entire Au-6 Voronoi grid with thermal electrons. We assume solar metallicity, and cosmic ray ionization rates and an interstellar radiation field (ISRF) that is representative of the Milky Way [18]. Note that we neglect the population of old field stars in our analysis, because they do not contribute to the ISRF at ionizing frequencies. The resulting distribution of free electrons agrees very well with the observationally-inspired models for the Milky Way by Cordes & Lazio [8] and by Yao et al. [41]. This is illustrated in Figure 8 of P21. For a detailed description of the magnetic field structure of the Auriga-6 galaxy, we refer to Pakmor et al. [26]. With this approach, we have all necessary information to compute the integral (2) through arbitrary sightlines through the galaxy.

Finally, we employ the radiative transfer (RT) code POLARIS[2] [34] capable of dust polarization calculations [33] as well as Zeeman splitting line RT [5, 33] and solve the RT problem on the native Voronoi grid of AREPO simulations. We calculate the resulting synthetic Faraday RM all-sky maps from ten selected positions in the Au-6 galaxy integrating equation (2) for many different sightlines across the entire galaxy and covering the entire sky with high angular resolution [35]. For our calculations of the synthetic RM maps we apply a HEALPIX[3] resolution of $N_{\rm side} = 256$ leading to a total amount of 786 432 pixel. This resolution is identical to the observed H22 map [16] but larger than O12 map by a factor of four. The location of the fictitious observers in the Au-6 galaxy are selected such that the distance to the galactic center is between 8 kpc and 10 kpc, with the solar values being 8.5 kpc, and that they are placed in a Local Bubble like region, where previous supernovae have created a low-density cavity, as illustrated in Figure 6 of P21.

[1] http://www.nublado.org/

[2] http://www1.astrophysik.uni-kiel.de/∼polaris/

[3] http://healpix.jpl.nasa.gov

Code Availability

Cluster properties and ionizaiton are calulated with the WARPFIELD code [31, 32] and the spectral synthesis code CLOUDY v17.00 (http://www.nublado.org/), respectively. Cosmological simulations are performed by the moving mesh code AREPO [39] (https://arepo-code.org/wp-content/userguide/index.html) and the RT post-processing we utilize the RT code POLARIS [34] (https://portia.astrophysik.uni-kiel.de/polaris/). We used Python and its associated libraries including ASTROPY, NUMPY, and MATPLOTLIB for data analysis and presentation.

Corresponding Author

The corresponding author is Stefan Reissl. Please send any requests for further information or data to `reissl@uni-heidelberg.de`.

Acknowledgements

S.R., R.S.K., E.W.P., and D.R. acknowledge support from the Deutsche Forschungsgemeinschaft in the Collaborative Research Center (SFB 881, ID 138713538) "The Milky Way System" (subprojects A1, B1, B2, and B8) and from the Heidelberg Cluster of Excellence (EXC 2181, ID 390900948) "STRUCTURES: A unifying approach to emergent phenomena in the physical world, mathematics, and complex data", funded by the German Excellence Strategy. R.S.K. also thanks for funding form the European Research Council in the ERC Synergy Grant "ECOGAL – Understanding our Galactic ecosystem: From the disk of the Milky Way to the formation sites of stars and planets" (ID 855130). RG acknowledges support from an STFC Ernest Rutherford Fellowship (ST/W003643/1)." F.A.G. acknowledges financial support from CONICYT through the project FONDECYT Regular Nr. 1181264, and funding from the Max Planck Society through a Partner Group grant. The project benefited from computing resources provided by the State of Baden-Württemberg through bwHPC and DFG through grant INST 35/1134-1 FUGG, and from the data storage facility SDS@hd supported through grant INST 35/1314-1 FUGG. The Heidelberg team also thank for computing time provided by the Leibniz Computing Center (LRZ) for project pr74nu.

Author Contributions

S.R. has run all polarized radiative transfer calculations and has performed most of the analysis. The text was jointly written by S.R. and R.S.K. The WARPFIELD cloud-cluster evolution model was mostly contributed by E.W.P. and D.R. The Augiga-6 data and support with the data handling have been provided by R.P., R.G., F.G., F.M., and V.S.

References

[1] M. I. R. Alves, F. Boulanger, K. Ferrière, and L. Montier. The Local Bubble: a magnetic veil to our Galaxy. *A&A*, 611:L5, April 2018.

[2] B.-G. Andersson, A. Lazarian, and J. E. Vaillancourt. Interstellar Dust Grain Alignment. *ARA&A*, 53:501–539, August 2015.

[3] M. C. Beck, A. M. Beck, R. Beck, K. Dolag, A. W. Strong, and P. Nielaba. New constraints on modelling the random magnetic field of the MW. *JCAP*, 5:056, May 2016.

[4] R. Beck. Magnetic fields in spiral galaxies. *A&ARv*, 24:4, December 2015.

[5] R. Brauer, S. Wolf, S. Reissl, and F. Ober. Magnetic fields in molecular clouds: Limitations of the analysis of Zeeman observations. *A&A*, 601:A90, May 2017.

[6] B. J. Burn. On the depolarization of discrete radio sources by Faraday dispersion. *MNRAS*, 133:67, 1966.

[7] I. Butsky, J. Zrake, J.-h. Kim, H.-I. Yang, and T. Abel. Ab Initio Simulations of a Supernova-driven Galactic Dynamo in an Isolated Disk Galaxy. *ApJ*, 843:113, July 2017.

[8] J. M. Cordes and T. J. W. Lazio. NE2001.I. A New Model for the Galactic Distribution of Free Electrons and its Fluctuations. *ArXiv Astrophysics e-prints*, July 2002.

[9] R. M. Crutcher. Magnetic Fields in Molecular Clouds: Observations Confront Theory. *ApJ*, 520:706, August 1999.

[10] G. J. Ferland, M. Chatzikos, F. Guzmán, M. L. Lykins, P. A. M. van Hoof, R. J. R. Williams, N. P. Abel, N. R. Badnell, F. P. Keenan, R. L. Porter, and P. C. Stancil. The 2017 Release Cloudy. *RMXAA*, 53:385, October 2017.

[11] K. M. Ferrière. The interstellar environment of our galaxy. *RvMP*, 73:1031, October 2001.

[12] R. J. J. Grand, F. A. Gómez, F. Marinacci, R. Pakmor, V. Springel, D. J. R. Campbell, C. S. Frenk, A. Jenkins, and S. D. M. White. The Auriga Project: the properties and formation mechanisms of disc galaxies across cosmic time. *MNRAS*, 467:179, May 2017.

[13] C. Heiles and M. Haverkorn. Magnetic Fields in the Multiphase Interstellar Medium. *SSRv*, 166:293, May 2012.

[14] P. Hennebelle. The FRIGG project: From intermediate galactic scales to self-gravitating cores. *A&A*, 611:A24, March 2018.

[15] S. Hutschenreuter, C. S. Anderson, S. Betti, G. C. Bower, J. A. Brown, M. Brüggen, E. Carretti, T. Clarke, A. Clegg, A. Costa, S. Croft, C. V. Eck, B. M. Gaensler, F. de Gasperin, M. Haverkorn, G. Heald, C. L. H. Hull, M. Inoue, M. Johnston-Hollitt, J. Kaczmarek, C. Law, Y. K. Ma, D. MacMahon, S. A. Mao, C. Riseley, S. Roy, R. Shanahan, T. Shimwell, J. Stil, C. Sobey, S. P. O'Sullivan, C. Tasse, V. Vacca, T. Vernstrom, P. K. G. Williams, M. Wright, and T. A. Enßlin. The Galactic Faraday rotation sky 2020. *A&A*, 657:A43, January 2022.

[16] Sebastian Hutschenreuter and Torsten A. Enßlin. The Galactic Faraday depth sky revisited. *A&A*, 633:A150, January 2020.

[17] R. C. Kennicutt. Star Formation in Galaxies Along the Hubble Sequence. *ARA&A*, 36:189, 1998.

[18] R. S. Klessen and S. C. O. Glover. Physical Processes in the Interstellar Medium. *Star Formation in Galaxy Evolution: Connecting Numerical Models to Reality, Saas-Fee Advanced Course, Volume 43. ISBN 978-3-662-47889-9. Springer-Verlag Berlin Heidelberg, 2016, p. 85*, 43:85, 2016.

[19] Mark R. Krumholz, Christopher F. McKee, and Joss Bland-Hawthorn. Star Clusters Across Cosmic Time. *ARA&A*, 57:227–303, August 2019.

[20] A. Lazarian, K. H. Yuen, H. Lee, and J. Cho. Synchrotron Intensity Gradients as Tracers of Interstellar Magnetic Fields. *ApJ*, 842:30, June 2017.

[21] S. A. Mao, C. Carilli, B. M. Gaensler, O. Wucknitz, C. Keeton, A. Basu, R. Beck, P. P. Kronberg, and E. Zweibel. Detection of microgauss coherent magnetic fields in a galaxy five billion years ago. *Nature Astronomy*, 1:621, August 2017.

[22] Christopher F. McKee and Eve C. Ostriker. Theory of Star Formation. *ARA&A*, 45(1):565–687, September 2007.

[23] D. Morris and G. L. Berge. Direction of the Galactic Magnetic Field in the Vicinity of the Sun. *ApJ*, 139:1388, May 1964.

[24] N. Oppermann, H. Junklewitz, G. Robbers, M. R. Bell, T. A. Enßlin, A. Bonafede, R. Braun, J. C. Brown, T. E. Clarke, I. J. Feain, B. M. Gaensler, A. Hammond, L. Harvey-Smith, G. Heald, M. Johnston-Hollitt, U. Klein, P. P. Kronberg, S. A. Mao, N. M. McClure-Griffiths, S. P. O'Sullivan, L. Pratley, T. Robishaw, S. Roy, D. H. F. M. Schnitzeler, C. Sotomayor-Beltran, J. Stevens, J. M. Stil, C. Sunstrum, A. Tanna, A. R. Taylor, and C. L. Van Eck. An improved map of the Galactic Faraday sky. *A&A*, 542:A93, June 2012.

[25] R. Pakmor, F. Marinacci, and V. Springel. Magnetic Fields in Cosmological Simulations of Disk Galaxies. *ApJ*, 783:L20, March 2014.

[26] Rüdiger Pakmor, Facundo A. Gómez, Robert J. J. Grand, Federico Marinacci, Christine M. Simpson, Volker Springel, David J. R. Campbell, Carlos S. Frenk, Thomas Guillet, Christoph Pfrommer, and Simon D. M. White. Magnetic field formation in the Milky Way like disc galaxies of the Auriga project. *MNRAS*, 469(3):3185–3199, August 2017.

[27] Rüdiger Pakmor, Thomas Guillet, Christoph Pfrommer, Facundo A. Gómez, Robert J. J. Grand, Federico Marinacci, Christine M. Simpson, and Volker Springel. Faraday rotation maps of disc galaxies. *MNRAS*, 481(4):4410–4418, December 2018.

[28] E. W. Pellegrini, D. Rahner, S. Reissl, S. C. O. Glover, R. S. Klessen, L. Rousseau-Nepton, and R. Herrera-Camus. WARPFIELD-EMP: The self-consistent prediction of emission lines from evolving H II regions in dense molecular clouds. *MNRAS*, 496(1):339–363, July 2020.

[29] Eric W. Pellegrini, Stefan Reissl, Daniel Rahner, Ralf S. Klessen, Simon C. O. Glover, Rüdiger Pakmor, Rodrigo Herrera-Camus, and Robert J. J. Grand. WARPFIELD population synthesis: the physics of (extra-)Galactic star formation and feedback-driven cloud structure and emission from sub-to-kpc scales. *MNRAS*, 498(3):3193–3214, November 2020.

[30] Planck Collaboration, P. A. R. Ade, N. Aghanim, M. I. R. Alves, M. Arnaud, D. Arzoumanian, M. Ashdown, J. Aumont, C. Baccigalupi, A. J. Banday, R. B. Barreiro, N. Bartolo, E. Battaner, K. Benabed, A. Benoît, A. Benoit-Lévy, J.-P. Bernard, M. Bersanelli, P. Bielewicz, J. J. Bock, L. Bonavera, J. R. Bond, J. Borrill, F. R. Bouchet, F. Boulanger, A. Bracco, C. Burigana, E. Calabrese, J.-F. Cardoso, A. Catalano, H. C. Chiang, P. R. Christensen, L. P. L. Colombo, C. Combet, F. Couchot, B. P. Crill, A. Curto, F. Cuttaia, L. Danese, R. D. Davies, R. J. Davis, P. de Bernardis, A. de Rosa, G. de Zotti, J. Delabrouille, C. Dickinson, J. M. Diego, H. Dole, S. Donzelli, O. Doré, M. Douspis, A. Ducout, X. Dupac, G. Efstathiou, F. Elsner, T. A. Enßlin, H. K. Eriksen, D. Falceta-Gonçalves, E. Falgarone, K. Ferrière, F. Finelli, O. Forni, M. Frailis, A. A. Fraisse, E. Franceschi, A. Frejsel, S. Galeotta, S. Galli, K. Ganga, T. Ghosh, M. Giard, E. Gjerløw, J. González-Nuevo, K. M. Górski, A. Gregorio, A. Gruppuso, J. E. Gudmundsson, V. Guillet, D. L. Harrison, G. Helou, P. Hennebelle, S. Henrot-Versillé, C. Hernández-Monteagudo, D. Herranz, S. R. Hildebrandt, E. Hivon, W. A. Holmes, A. Hornstrup, K. M. Huffenberger, G. Hurier, A. H. Jaffe, T. R. Jaffe, W. C. Jones, M. Juvela, E. Keihänen, R. Keskitalo, T. S. Kisner, J. Knoche, M. Kunz, H. Kurki-Suonio, G. Lagache, J.-M. Lamarre, A. Lasenby, M. Lattanzi, C. R. Lawrence, R. Leonardi, F. Levrier, M. Liguori, P. B. Lilje, M. Linden-Vørnle, M. López-Caniego, P. M. Lubin, J. F. Macías-Pérez, D. Maino, N. Mandolesi, A. Mangilli, M. Maris, P. G. Martin, E. Martínez-González, S. Masi, S. Matarrese, A. Melchiorri, L. Mendes, A. Mennella,

M. Migliaccio, M.-A. Miville-Deschênes, A. Moneti, L. Montier, G. Morgante, D. Mortlock, D. Munshi, J. A. Murphy, P. Naselsky, F. Nati, C. B. Netterfield, F. Noviello, D. Novikov, I. Novikov, N. Oppermann, C. A. Oxborrow, L. Pagano, F. Pajot, R. Paladini, D. Paoletti, F. Pasian, L. Perotto, V. Pettorino, F. Piacentini, M. Piat, E. Pierpaoli, D. Pietrobon, S. Plaszczynski, E. Pointecouteau, G. Polenta, N. Ponthieu, G. W. Pratt, S. Prunet, J.-L. Puget, J. P. Rachen, M. Reinecke, M. Remazeilles, C. Renault, A. Renzi, I. Ristorcelli, G. Rocha, M. Rossetti, G. Roudier, J. A. Rubiño-Martín, B. Rusholme, M. Sandri, D. Santos, M. Savelainen, G. Savini, D. Scott, J. D. Soler, V. Stolyarov, R. Sudiwala, D. Sutton, A.-S. Suur-Uski, J.-F. Sygnet, J. A. Tauber, L. Terenzi, L. Toffolatti, M. Tomasi, M. Tristram, M. Tucci, G. Umana, L. Valenziano, J. Valiviita, B. Van Tent, P. Vielva, F. Villa, L. A. Wade, B. D. Wandelt, I. K. Wehus, N. Ysard, D. Yvon, and A. Zonca. Planck intermediate results. XXXV. Probing the role of the magnetic field in the formation of structure in molecular clouds. *A&A*, 586:A138, February 2016.

[31] Daniel Rahner, Eric W. Pellegrini, Simon C. O. Glover, and Ralf S. Klessen. Winds and radiation in unison: a new semi-analytic feedback model for cloud dissolution. *MNRAS*, 470:4453, 2017.

[32] Daniel Rahner, Eric W. Pellegrini, Simon C. O. Glover, and Ralf S. Klessen. WARPFIELD 2.0: feedback-regulated minimum star formation efficiencies of giant molecular clouds. *MNRAS*, 483(2):2547–2560, February 2019.

[33] S. Reissl, A. M. Stutz, R. Brauer, E. W. Pellegrini, D. R. G. Schleicher, and R. S. Klessen. Magnetic fields in star-forming systems (I): idealized synthetic signatures of dust polarization and Zeeman splitting in filaments. *MNRAS*, 481:2507, December 2018.

[34] S. Reissl, S. Wolf, and R. Brauer. Radiative transfer with POLARIS. I.: Analysis of magnetic fields through synthetic dust continuum polarization measurements. *A&A*, 593:A87, September 2016.

[35] Stefan Reissl, Robert Brauer, Ralf S. Klessen, and Eric W. Pellegrini. Radiative Transfer with POLARIS. II.: Modeling of Synthetic Galactic Synchrotron Observations. *ApJ*, 885(1):15, November 2019.

[36] M. Rieder and R. Teyssier. A small-scale dynamo in feedback-dominated galaxies as the origin of cosmic magnetic fields - I. The kinematic phase. *MNRAS*, 457:1722, April 2016.

[37] G. B. Rybicki and A. P. Lightman. *Radiative processes in astrophysics*. 1979.

[38] R. Shanahan, S. J. Lemmer, J. M. Stil, H. Beuther, Y. Wang, J. Soler, L. D. Anderson, F. Bigiel, S. C. O. Glover, P. Goldsmith, R. S. Klessen, N. M.

McClure-Griffiths, S. Reissl, M. Rugel, and R. J. Smith. Strong Excess Faraday Rotation on the Inside of the Sagittarius Spiral Arm. *APJL*, 887(1):L7, December 2019.

[39] V. Springel. E pur si muove: Galilean-invariant cosmological hydrodynamical simulations on a moving mesh. *MNRAS*, 401:791, January 2010.

[40] X. H. Sun, T. L. Landecker, B. M. Gaensler, E. Carretti, W. Reich, J. P. Leahy, N. M. McClure-Griffiths, R. M. Crocker, M. Wolleben, M. Haverkorn, K. A. Douglas, and A. D. Gray. Faraday Tomography of the North Polar Spur: Constraints on the Distance to the Spur and on the Magnetic Field of the Galaxy. *ApJ*, 811:40, September 2015.

[41] J. M. Yao, R. N. Manchester, and N. Wang. A New Electron-density Model for Estimation of Pulsar and FRB Distances. *ApJ*, 835(1):29, January 2017.

[42] Catherine Zucker, Alyssa A. Goodman, João Alves, Shmuel Bialy, Michael Foley, Joshua S. Speagle, Josefa Groschedl, Douglas P. Finkbeiner, Andreas Burkert, Diana Khimey, and Cameren Swiggum. Star formation near the Sun is driven by expansion of the Local Bubble. *Nature*, 601(7893):334–337, January 2022.